Beam-Pattern Assisted Low-Complexity Beam Alignment for Fixed Wireless mmWave xHaul

Jun Qian[1], Christos Masouros[1], Kosuke Tanabe[2], Eisaku Sasaki[2], Nader Zein[3], Tsunehisa Marumoto[2]
[1]University College London, London, UK, emails: {jun.qian.15, c.masouros}@ucl.ac.uk
[2]NEC Corporation, Kawasaki, Japan, emails: {k.tanabe, sasaki-e, marumoto}@nec.com
[3]NEC Europe Ltd., London, UK, email: nader.zein@emea.nec.com

***Abstract*—This paper presents the design of two-stage beam alignment methods employing a hybrid analog-digital antenna array and exploiting the beam pattern in a point-to-point millimeter-wave (mmWave) radio for mmWave massive multiple-input multiple-output systems. We investigate an antenna deactivating approach that generates wider beams at the coarse alignment stage and exploit the theoretical beam pattern at the fine alignment stage. Our numerical results show that the proposed two-stage methods can achieve a better beam alignment than existing exhaustive methods and avail measurements/complexity reductions by tuning key parameters governing the alignment performance.**

***Index Terms*—Antenna Gain, Beam Alignment, mmWave, Massive MIMO**

I. Introduction

Millimeter-Wave (mmWave) communication has attracted intense research interest due to the large spectrum bands available at the mmWave frequencies, that have the potential of high data rates [1]–[3]. However, the increased path loss poses a challenge for mmWave communications. To compensate for this challenge, high-gain beamforming together with accurate transmitter (Tx) and receiver (Rx) beam alignment is required to acquire large antenna gains [4].

Theoretical beam alignment techniques for mmWave systems to achieve high antenna gains have been developed in previous studies. The work in [5] has studied hard-alignment algorithms for uniform linear array (ULA) scenarios, while a soft-alignment algorithm scanning the channel subspace with dual-polarized antennas has been presented in [4]. Hierarchical codebook design with ULA arrays has been illustrated in [6], and [7] also proposed wider beams to speed up beam scanning. The beam alignment techniques presented in [8], [9] can investigate the promising channel estimation performance of the angle of departure (AoD) and angle of arrival (AoA) in single-user ULA mmWave system. A conventional approach to adjust Tx and Rx beams jointly is performing an exhaustive method by examining all potential beam pairs [10]. However, this consumes significant computational complexity and signalling overheads when a large number of beam pairs are steered or suffers gain losses if the scan interval is large.

This work focuses on a detailed electromagnetic simulation of the antenna arrays at the Tx and Rx, and proposes two-stage alignment methods starting with wider beams achieved by deactivating antennas at the Tx and Rx to speed up beam scanning, and then refined with a precise estimate of the direction range. To further achieve low-complexity beam alignment, we exploit the knowledge of the beam patterns to identify the optimal alignment directions with only minimal additional samples. This attains both required performance and potential measurement/complexity reduction. Our method is supported by the steerable, hybrid antenna array architecture of massive multiple-input multiple-output (MIMO) Tx and Rx. Numerical results demonstrate the effectiveness for complexity reduction of our proposed alignment methods under the experimental scenario.

This work was supported by NEC Laboratories Europe GmbH.

II. System model

A. Free Space Propagation Model

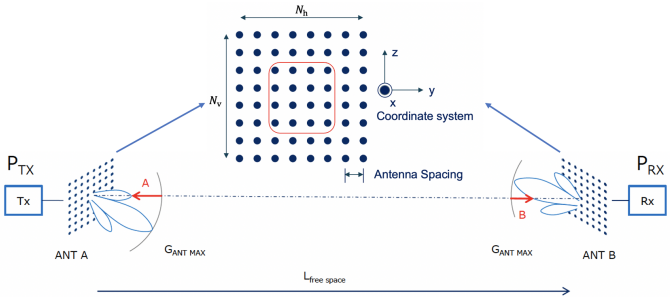

Fig. 1: Free Space Communication Link with yz-plane planar array

A point-to-point fixed wireless mmWave communication link is shown in Fig. 1, dominated by a strong line-of-sight (LOS) component [5]. To simplify our electromagnetic simulation, we employ the free space propagation model to model the LOS path in a free space environment between the Tx and Rx. We assume that the Tx and Rx antennas are matched in impedance to their connecting transmission lines [11], [12]. The received signal power in free space at a distance R from the Tx can be expressed in form of the Friis formulation [3], [13]

$$P_{Rx} = P_{Tx}\frac{G_{Tx}G_{Rx}\lambda^2}{(4\pi R)^2}, \tag{1}$$

where P_{Rx} and P_{Tx} are the received power and transmit power. G_{Rx} and G_{Tx} are the receive and transmit antenna gains. R is the Tx-Rx separation distance and $\lambda = c/f$ is

the carrier wavelength with f, the mmWave frequency, and $c = 3 \times 10^8\ m/s$, the speed of light. A dB-form reads as

$$P_{Rx}(\text{dBm}) = P_{Tx}(\text{dBm}) + G_{Tx}(\text{dB}) + G_{Rx}(\text{dB}) - 20\log R(\text{km}) - 20\log f(\text{MHz}) - 32.44, \tag{2}$$

where, $\text{L}_{\text{free space}} = -20\log R(\text{km}) - 20\log f(\text{MHz}) - 32.44$ is the free space path loss. To validate the communication link, the actual received power should be larger than the minimum required received signal level, and the gap between these two factors is the link margin [11], [12]. As shown in Fig. 1, $G_{ANT}^{TX}\ (dB)$ and $G_{ANT}^{RX}\ (dB)$ are optimal gains with $G_{opt}\ (dB) = G_{ANT}^{TX}\ (dB) + G_{ANT}^{RX}\ (dB)$, $A + B$ is the gain loss caused by misalignment. In our studies, the target is to achieve close-to-optimal antenna gain and improve $G\ (dB) = G_{Tx}\ (dB) + G_{Rx}\ (dB) = G_{opt}\ (dB) - (A + B)$.

B. Antenna Array and Antenna Gain

We define the array factor as $AF(\theta, \phi)$ in massive MIMO antenna arrays, where (θ, ϕ) denotes the angle coordinates of elevation and azimuth directions of AoD/AoA. By controlling the progressive phase excitation between antennas, the maximum radiation can be targeted toward in the desired direction to form a scanning array and achieve beam alignment [11], [14]. We assume that each antenna element is excited with a signal at an amplitude of one and a varying phase shift. Thus, the phase-shifted array factor of the $N_v \times N_h$ uniform planar array (UPA) is expressed as [11], [12], [15]

$$AF(\theta, \phi) = \sum\nolimits_{n=1}^{N_h} \sum\nolimits_{m=1}^{N_v} e^{j(2\pi \hat{\mathbf{r}} \cdot \mathbf{r}_{mn} + \beta_{mn})}. \tag{3}$$

Here, β_{mn} is the phase excitation of the mn-th antenna. N_v and N_h are the number of the vertical and horizontal antennas respectively. $\hat{\mathbf{r}}$ is the unit vector pointing in AoD/AoA [11], [12]:

$$\hat{\mathbf{r}} = \sin\theta\cos\phi\hat{\mathbf{x}} + \sin\theta\sin\phi\hat{\mathbf{y}} + \cos\theta\hat{\mathbf{z}}. \tag{4}$$

The antennas for a three-dimensional array are located with position vectors normalised by carrier wavelength from the origin to the mn-th antenna:

$$\mathbf{r}_{mn} = x_{mn}\hat{\mathbf{x}} + y_{mn}\hat{\mathbf{y}} + z_{mn}\hat{\mathbf{z}}. \tag{5}$$

Fig. 1 shows a UPA example with antennas arranged uniformly along a rectangular grid in the yz-plane [11], [12]. Moreover, z is the elevation direction and y is the azimuth direction. The phase-shifted array factor of yz-plane UPA is expanded to

$$AF(\theta, \phi) = \sum\nolimits_{n=1}^{N_h} \sum\nolimits_{m=1}^{N_v} e^{j2\pi(y_{mn}\sin\theta\sin\phi + z_{mn}\cos\theta - y_{mn}\sin\theta_0\sin\phi_0 - z_{mn}\cos\theta_0)}. \tag{6}$$

where θ_0 and ϕ_0 are the elevation and azimuth phase excitation achieved by Intermediate Frequency (IF) phase control in mmWave radio unit. For simplicity, we assume $N_v = N_h = N$ in the following studies.

Typically, the field pattern of an actual antenna is defined as a product of an element factor and a pattern factor. Then, the complete array pattern can be acquired by the product of the element pattern and the phase-shifted array factor [11], [12]

$$F(\theta, \phi) = g(\theta, \phi)AF(\theta, \phi). \tag{7}$$

Here, the element pattern provided by the experimental mmWave radio unit is

$$g(\theta, \phi) = -\min\Big[12(\frac{\cos^{-1}(\cos\theta\sin\phi)}{\mathcal{B}})^2, \mathcal{S}\Big], \tag{8}$$

where, $\mathcal{B} = 50.8/(Nd)$ is the half-power beamwidth (HPBW) with inter-antenna distance d normalised by λ. $\mathcal{S}$ is the sidelobe level (SLL) introducing how large is the ratio of the side lobe compared to the main lobe [14], [16]

$$\mathcal{S} = 20 \cdot 1\log_{10}\Big(\frac{\text{the maximum value of largest side lobe}}{\text{the maximum value of main lobe}}\Big). \tag{9}$$

The antenna gain, applied in the communication link, is defined as 4π times the ratio of the radiation intensity in a given direction to the power input by the antenna [11], [14]. The total radiated power is related to the total input power by $P_{rad} = k \cdot P_{in}$. Then, the gain can be given by

$$G(\theta, \phi) = 4\pi\frac{U(\theta, \phi)}{P_{in}}, \tag{10}$$

where $U(\theta, \phi) = |F(\theta, \phi)|^2$ is the radiation intensity in terms of the power radiated from an antenna per unit solid angle [11], [12]. P_{rad} is the total radiated power expressed as

$$P_{rad} = \int_0^{2\pi}\int_0^{\pi} U(\theta, \phi)sin(\theta)d\theta d\phi. \tag{11}$$

Then, (10) can be re-written as

$$G(\theta, \phi) = k \cdot 4\pi\frac{U(\theta, \phi)}{\int_0^{2\pi}\int_0^{\pi} U(\theta, \phi)sin(\theta)d\theta d\phi}, \tag{12}$$

where k is the antenna radiation efficiency. For simplicity, we assume $k = 1$. Later, 10 log would be applied to acquire the dB-form antenna gain.

III. Two-stage Beam Alignment Methods

In this paper, we propose the design of two-stage alignment methods by exploiting an antenna deactivating strategy and the beam pattern [6], [17]. Before the method design, we first introduce the key techniques applied in the design.

1) Deactivating Approach: As shown in Fig. 1, we assume $N \times N$-element antenna arrays with $N_h = N_v = N$ in yz-plane for both Tx and Rx. The antenna-position vectors for yz-plane planar array can be extended to

$$\mathbf{r}_{mn} = y_{mn}\hat{\mathbf{y}} + z_{mn}\hat{\mathbf{z}}, m = 1, ..., N, n = 1, ..., N, \tag{13}$$

where y_{mn} and z_{mn} are the mn-th elements in $\mathbf{y} . * \mathbf{I}_N$ and $\mathbf{z} . * \mathbf{I}_N$, respectively. Since the origin is the center $(0, 0)$, then, the initial position coordinates $\mathbf{y} = \mathbf{z} = \mathbf{P} \in \mathbb{C}^{1\times N}$ can be given by

$$\mathbf{P} = 2d \cdot [-(N-1), -(N-3), ..., (N-1)], \tag{14}$$

where d is the normalised inter-antenna distance. If $N_{active} \times N_{active}$ antennas are active for beam scanning with $N_{active} \leq N$, the position coordinates of active antennas can be given by

$$\mathbf{P}_{active} = \mathbf{P}(5 + \frac{\epsilon - N_{active}}{2} : 4 + \frac{\epsilon + N_{active}}{2}), \tag{15}$$

where, $\epsilon = \lceil N_{active} \rceil - \lfloor N_{active} \rfloor$. Thus, $\mathbf{y}_{active} = \mathbf{z}_{active} = \mathbf{P}_{active}$ will acquire the position vectors of active antennas.

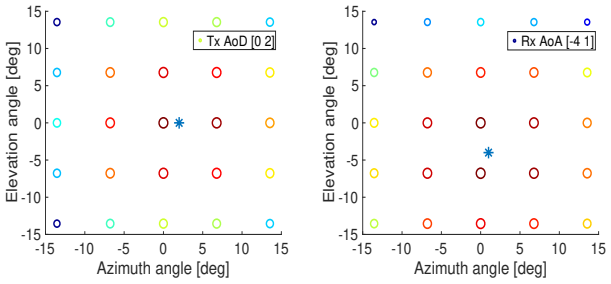

Fig. 2: Scan range in square grid array, $N_{active} = 6$, initial scan range $= [-15, 15]$, scan interval $= 0.4 \cdot \mathcal{B}$, stars are the optimal AoD/AoA.

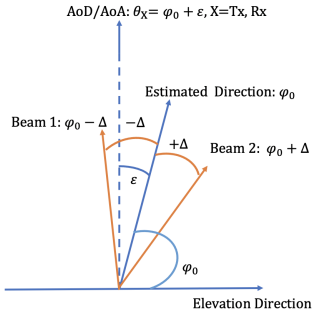

Fig. 3: S-curve generation of elevation direction

2) Scanning Approach: It is assumed that the link's optimal AoD (θ_{Tx}, ϕ_{Tx}) and AoA (θ_{Rx}, ϕ_{Rx}) remain constant at Tx and Rx during the alignment, we steer the phase excitation within the given scan range to match the optimal AoD and AoA. The angle variables (φ^X, μ^X) represents the phase excitation, and the initial elevation and azimuth scan ranges are defined as $[-\varphi_X, \varphi_X]$ and $[-\mu_X, \mu_X]$, $X = Tx,\ Rx$. The scan interval is $a{\cdot}\mathcal{B}$ to determine the coordinates of scanning points with a, the interval parameter. Fig. 2 shows an example of the scan range distribution. The empty circles are the coordinates of phase excitation (φ^X, μ^X) with relevant gain $G_X(\varphi^X, \mu^X)$, $X = Tx,\ Rx$. The scan approach generating the table matrices is given by

Step 1: Define the Tx table matrix as $\mathbf{H}_{Tx} \in \mathbb{C}^{M_{Tx}\times 3}$. $M_{Tx} = M_\varphi^{Tx} M_\mu^{Tx}$ is the total number of scanning points and M_φ^{Tx} and M_μ^{Tx} are the number of elevation and azimuth phase excitation. Based on the coordinate of scanning point $(\varphi_i^{Tx}, \mu_j^{Tx})$ and its antenna gain $G_{Tx}(\varphi_i^{Tx}, \mu_j^{Tx})$, $i = 1, ..., M_\varphi^{Tx}$, $j = 1, ..., M_\mu^{Tx}$, the generation process can be instructed by Algorithm 1.

Step 2: Define the Rx table matrix as $\mathbf{H}_{Rx} \in \mathbb{C}^{M_{Rx}\times 3}$. $M_{Rx} = M_\varphi^{Rx} M_\mu^{Rx}$ is the total number of scanning points and M_φ^{Rx} and M_μ^{Rx} are the number of elevation and azimuth phase excitation. Based on the coordinate of scanning point $(\varphi_i^{Rx}, \mu_j^{Rx})$ and its antenna gain $G_{Rx}(\varphi_i^{Rx}, \mu_j^{Rx})$, $i = 1, ..., M_\varphi^{Rx}$, $j = 1, ..., M_\mu^{Rx}$, the generation process is instructed by Algorithm 1.

Step 3: Now we focus on $G\ (dB) = G_{Tx}\ (dB) + G_{Rx}\ (dB)$. If we observe Tx with a specific phase excitation $(\varphi_i^{Tx}, \mu_j^{Tx})$, all phase excitation at Rx, namely, M_{Rx} scanning point pairs will be steered to select the phase excitation pair achieving the maximum $G\ (dB)$. This process will be repeated for all phase excitation at Tx; thus, an updated table matrix $\mathbf{H}_{Tx}^{\text{up}} \in \mathbb{C}^{M_{Tx}\times 7}$ will be obtained, which is further instructed by Algorithm 1.

Step 4: Similarly, if we observe Rx with a fixed phase excitation $(\varphi_i^{Rx}, \mu_j^{Rx})$, we will scan all phase excitation at Tx to steer M_{Tx} scanning point pairs for the phase excitation pair selection achieving maximum $G\ (dB)$. This process will be repeated for all phase excitation at Rx; thus, an updated table matrix $\mathbf{H}_{Rx}^{\text{up}} \in \mathbb{C}^{M_{Rx}\times 7}$ will be obtained based on Algorithm 1.

Step 5: With the aid of updated table matrices, we can find the specific Tx and Rx phase excitation to achieve the maximum gain or the narrowed range where the optimal AoD and AoA are located to promote the beam alignment.

3) S-curve Generation: The gain difference between adjacent beams can be obtained off-line using the theoretical beam patterns produced by the Tx or Rx arrays. Owing to its shape, we denote this theoretical function as the *S-curve*. The S-curve is one-dimensional; thus, we have to obtain the separate elevation and azimuth S-curves. We take the elevation S-curve generation in Fig. 3 as an example, where the estimated elevation direction is φ_0 and the angle error between φ_0 and the optimal AoD/AoA is ε with $\theta_X = \varphi_0 + \varepsilon$, $X = Tx, Rx$. Two beams are sampled with measured gains $G(\varphi_0 + \Delta, \mu)(dB)$ and $G(\varphi_0 - \Delta, \mu)(dB)$, where Δ is the sample interval. Thus, the S-curve can be obtained as a function of ε by calculating the gain difference between the two sampled beams,

$$\begin{aligned} G_{diff}(\varepsilon)\ (dB) &= G(\varphi_0 + \Delta, \mu^X)\ (dB) - G(\varphi_0 - \Delta, \mu^X)\ (dB) \\ &= G(\theta_X - \varepsilon + \Delta, \mu^X)\ (dB) - G(\theta_X - \varepsilon - \Delta, \mu^X)\ (dB), \end{aligned} \tag{16}$$

where $X = Tx,\ Rx$. The directions of these two sampled beams should be within the range of the main lobe to guarantee the alignment accuracy; thus, we can have the angle error range, $\varepsilon \in [\Delta - \mathcal{B}, \mathcal{B} - \Delta]$ with $0 < \Delta < \mathcal{B}$. The elevation and azimuth

Algorithm 1 Table matrix generation at Tx and Rx

Input: M_X, M_φ^X, M_μ^X, $\varphi_X \in \mathbb{C}^{M_\varphi^X \times 1}$, $\mu_X \in \mathbb{C}^{M_\mu^X \times 1}$, $X = Tx,\ Rx$.
Output: $\mathbf{H}_X \in \mathbb{C}^{M_X\times 3}$,$\mathbf{H}_X^{\text{up}} \in \mathbb{C}^{M_X\times 7}$, $X = Tx,\ Rx$.
Tx/Rx Table matrix:
kk = 0
for $i = 1 : M_\varphi^X$ **do**
  for $j = 1 : M_\mu^X$ **do**
    kk = kk + 1;
    $\mathbf{H}_X$(kk, 1) = $\varphi_X(i)$;
    $\mathbf{H}_X$(kk, 2) = $\mu_X(j)$;
    $\mathbf{H}_X$(kk, 3) = $10\log_{10} G_X(\varphi_i^X, \mu_j^X)$ supported by (12).
  end for
end for
Updated Table matrix:
$\mathbf{H}_X^{\text{up}}(:, 1:3) = \mathbf{H}_X$
for $i = 1 : M_X$ **do**
  $[m]$ = find($\mathbf{H}_X(i, 3) + \mathbf{H}_Y(:, 3)$ == max($\mathbf{H}_X(i, 3) + \mathbf{H}_Y(:, 3)$));
  $\mathbf{H}_X^{\text{up}}(i, 4:6) = \mathbf{H}_Y(m, :)$;
  $\mathbf{H}_X^{\text{up}}(i, 7) = \mathbf{H}_X(i, 3) + \mathbf{H}_Y(m, 3)$;
end for
Note: If $X = Tx$, $Y = Rx$, vice versa.

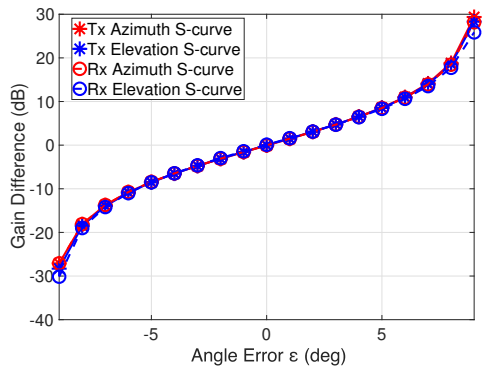

Fig. 4: S-Curve v.s. Angle error, AoD=[0 2] and AoA=[-4 1].

extensions of $G_{diff}(\varepsilon)$ referring to (6)-(12) in dB-form are given by

$$G^{\varphi}_{diff}(\varsigma) = 10\log_{10}\left(\frac{\sum_{m=1}^{N\times N}\sum_{n=1}^{N\times N} g_{+}(\varsigma)^2 e^{2\pi jNu_{\varphi,+\Delta}}}{\sum_{a=1}^{\text{length}(\hat{\theta})}\sum_{b=1}^{\text{length}(\hat{\phi})}\sum_{m=1}^{N\times N}\sum_{n=1}^{N\times N}\chi(a)g(a,b)^2 e^{2\pi jDe_{\varphi,+\Delta}}}\right) - 10\log_{10}\left(\frac{\sum_{m=1}^{N\times N}\sum_{n=1}^{N\times N} g_{-}(\varsigma)^2 e^{2\pi jNu_{\varphi,-\Delta}}}{\sum_{a=1}^{\text{length}(\hat{\theta})}\sum_{b=1}^{\text{length}(\hat{\phi})}\sum_{m=1}^{N\times N}\sum_{n=1}^{N\times N}\chi(a)g(a,b)^2 e^{2\pi jDe_{\varphi,-\Delta}}}\right), \tag{17}$$

$$G^{\mu}_{diff}(\varsigma) = 10\log_{10}\left(\frac{\sum_{m=1}^{N\times N}\sum_{n=1}^{N\times N} \gamma_{+}(\varsigma)^2 e^{2\pi jNu_{\mu,+\Delta}}}{\sum_{a=1}^{\text{length}(\hat{\theta})}\sum_{b=1}^{\text{length}(\hat{\phi})}\sum_{m=1}^{N\times N}\sum_{n=1}^{N\times N}\chi(a)g(a,b)^2 e^{2\pi jDe_{\mu,+\Delta}}}\right) - 10\log_{10}\left(\frac{\sum_{m=1}^{N\times N}\sum_{n=1}^{N\times N} \gamma_{-}(\varsigma)^2 e^{2\pi jNu_{\mu,-\Delta}}}{\sum_{a=1}^{\text{length}(\hat{\theta})}\sum_{b=1}^{\text{length}(\hat{\phi})}\sum_{m=1}^{N\times N}\sum_{n=1}^{N\times N}\chi(a)g(a,b)^2 e^{2\pi jDe_{\mu,-\Delta}}}\right), \tag{18}$$

with

$$Nu_{\varphi,\pm\Delta} = (\sin\theta_X\sin\phi_X - \sin(\theta_X - \varsigma \pm \Delta)\sin\mu^X)(\mathbf{y}(m) - \mathbf{y}(n)) + (\cos\theta_X - \cos(\theta_X - \varsigma \pm \Delta))(\mathbf{z}(m) - \mathbf{z}(n)), \tag{19}$$

$$De_{\varphi,\pm\Delta} = (\sin\hat{\theta}(a)\sin\hat{\phi}(b) - \sin(\theta_X - \varsigma \pm \Delta)\sin\mu^X)(\mathbf{y}(m) - \mathbf{y}(n)) + (\cos\hat{\theta}(a) - \cos(\theta_X - \varsigma \pm \Delta))(\mathbf{z}(m) - \mathbf{z}(n)), \tag{20}$$

$$Nu_{\mu,\pm\Delta} = (\sin\theta_X\sin\phi_X - \sin\varphi^X\sin(\phi_X - \varsigma \pm \Delta))(\mathbf{y}(m) - \mathbf{y}(n)) + (\cos\theta_X - \cos\varphi^X)(\mathbf{z}(m) - \mathbf{z}(n)), \tag{21}$$

$$De_{\mu,\pm\Delta} = (\sin\hat{\theta}(a)\sin\hat{\phi}(b) - \sin\varphi^X\sin(\phi_X - \varsigma \pm \Delta))(\mathbf{y}(m) - \mathbf{y}(n)) + (\cos\hat{\theta}(a) - \cos\varphi^X)(\mathbf{z}(m) - \mathbf{z}(n)). \tag{22}$$

The relevant element patterns in (17)-(18) are given by

$$g_{\pm}(\varepsilon) = -\min\Big[12(\frac{\cos^{-1}(\cos(\theta_X - \varepsilon \pm \Delta)\sin\mu^X)}{\mathcal{B}})^2, \mathcal{S}\Big], \tag{23}$$

$$\gamma_{\pm}(\varepsilon) = -\min\Big[12(\frac{\cos^{-1}(\cos\varphi^X\sin(\phi_X - \varepsilon \pm \Delta))}{\mathcal{B}})^2, \mathcal{S}\Big], \tag{24}$$

$$g(a,b) = -\min\Big[12(\frac{\cos^{-1}(\cos\hat{\theta}(a)\hat{\phi}(b))}{\mathcal{B}})^2, \mathcal{S}\Big]. \tag{25}$$

$\hat{\theta} \in (0,\pi)$ and $\hat{\phi} \in (-\pi/2, \pi/2)$ are applied for the total radiated power with respective intervals Δ_θ, Δ_ϕ, and $\chi(a) = \sin\hat{\theta}(a)\frac{\Delta_\theta\Delta_\phi(\pi/180)^2}{4\pi}$. Fig. 4 shows the example elevation and azimuth S-curves for AoD =[0 2] and AoA=[-4 1] as functions of the angle error ε (deg). Both elevation and azimuth S-curves share the same curve as we assume a symmetric antenna array at both the Tx and the Rx.

A. Dual-Deactivating Alignment Method (DD-BA)

In this method, deactivating approach is applied in both stages with the same number of active antennas.

1) Stage 1: The deactivating approach with $N_{active} \times N_{active}$ antennas is employed within the scan range of $[-\varphi_X, \varphi_X]$ and $[-\mu_X, \mu_X]$, $X = Tx,\ Rx$. The scan interval, $a \cdot \mathcal{B}_1$ with $\mathcal{B}_1 = 50.8/(N_{active}d)$, is applied to determine the scanning point coordinates. If the maximum antenna gain obtained in Stage 1 is G^1_{max} (dB), the narrowed scan range would be determined by selecting the phase excitation pairs with G $(dB) > G^1_{max}$ $(dB) - \delta$ (dB) referring to the table matrices, where δ (dB) is the threshold in the observed link gain to determine the narrowed scan range. Thus, the narrowed scan range can be $[\varphi^{\text{low}}_X, \varphi^{\text{upper}}_X]$ and $[\mu^{\text{low}}_X, \mu^{\text{upper}}_X]$, $X = Tx,\ Rx$.

2) Stage 2: Deactivating approach with $N_{active} \times N_{active}$ active antennas is still applied to complete the scanning within the narrowed scan range obtained by Stage 1. $b \cdot \mathcal{B}_2$ with $\mathcal{B}_2 = 50.8/(N_{active}d)$ is used as the scan interval to determine the new scanning points in Stage 2. After steering all scanning point pairs in Stage 2 and obtaining the table matrices of Stage 2, we can find the optimal angles of the Tx and Rx phase excitation. Then, all antennas are activated to point to the selected directions with maximum gain G_{max} (dB).

B. Deactivating S-curve Alignment Method (DS-BA)

In the DS-BA method, deactivating approach is applied in Stage 1. Then in Stage 2, we activate all antennas to exploit the above-mentioned S-curves for linear interpolation.

1) Stage 1: The scanning process is the same as Stage 1 in the DD-BA method, where $N_{active} \times N_{active}$ antennas are active for scanning. If the maximum antenna gain obtained in Stage 1 is G^1_{max} (dB); then the scanning points attaining G^1_{max} (dB), e.g., $(\varphi^{\text{stage1}}_{X,i}, \mu^{\text{stage1}}_{X,i})$ will be selected, $i = 1, ..., N_{p,X}$, where $N_{p,X}$ is the total number of scanning points achieving G^1_{max} (dB). An averaging method will be applied to obtain

$$\bar{\psi}^{\text{stage1}}_X = \frac{1}{N_{p,X}}\sum\nolimits_{i=1}^{N_{p,X}} \psi^{\text{stage1}}_{X,i}, \psi = \varphi, \mu, \tag{26}$$

where, $X = Tx,\ Rx$. $\bar{\varphi}^{\text{stage1}}_X$ and $\bar{\mu}^{\text{stage1}}_X$ will be used as the estimated directions for the S-curve interpolation in Stage 2.

2) Stage 2: All $N \times N$ antennas are active in this stage, and off-line elevation and azimuth S-curves are exploited to attain gain difference interpolation; thus, the process is:

Step 1: Calculate the elevation gain difference by G^{φ}_{diff} (dB) = $G(\bar{\varphi}^{\text{stage1}}_X + \Delta, \bar{\mu}^{\text{stage1}}_X)$ $(dB) - G(\bar{\varphi}^{\text{stage1}}_X - \Delta, \bar{\mu}^{\text{stage1}}_X)$ (dB).

Step 2: Interpolate G^{φ}_{diff} (dB) to the elevation S-curve via Matlab function interp1() to obtain the elevation angle error ε_φ and the achievable elevation direction is $\bar{\varphi}_X = \bar{\varphi}^{\text{stage1}}_X + \varepsilon_\varphi$.

Step 3: The azimuth gain difference can be obtained by $G^{\mu}_{diff}\ (dB) = G(\bar{\varphi}_X^{\text{stage1}}, \bar{\mu}_X^{\text{stage1}} + \Delta)\ (dB) - G(\bar{\varphi}_X^{\text{stage1}}, \bar{\mu}_X^{\text{stage1}} - \Delta)\ (dB)$.

Step 4: Interpolate $G^{\mu}_{diff}\ (dB)$ to the azimuth S-curve by Matlab function interp1() to obtain the azimuth angle error ε_μ and the achievable azimuth direction is $\bar{\mu}_X = \bar{\mu}_X^{\text{stage1}} + \varepsilon_\mu$.

Step 5: If $G(\bar{\varphi}_{Tx}, \bar{\mu}_{Tx})\ (dB) + G(\bar{\varphi}_{Rx}, \bar{\mu}_{Rx})\ (dB) < G_{opt}\ (dB) - \tau\ (dB)$, $(\bar{\varphi}_{Tx}, \bar{\mu}_{Tx})$ and $(\bar{\varphi}_{Rx}, \bar{\mu}_{Rx})$ will be used as estimated directions to repeat Step 1-4 until $G(\bar{\varphi}_{Tx}, \bar{\mu}_{Tx})\ (dB) + G(\bar{\varphi}_{Rx}, \bar{\mu}_{Rx})\ (dB) \geq G_{opt}\ (dB) - \tau\ (dB)$. This repetition might last for L times.

IV. Number of Measurements and Total Complexity

1) Number of Measurements: In Stage 1, we consider that one scanning point pair equates to one measurement. The predefined scan ranges are the same for both directions; thus, Tx and Rx have the same number of scanning points M_{scan}. The number of measurements in Stage 1 is M^2_{scan}. For DD-BA, the scan ranges are narrowed by the scanning in Stage 1; thus, both Tx and Rx have their respective number of scanning points in stage 2, which are, M_{Tx} and M_{Rx}. Thus, the number of total measurements of the DD-BA method is given by,

$$M_{total} = M^2_{scan} + M_{Tx} \cdot M_{Rx}. \tag{27}$$

For DS-BA, the gain difference interpolation employs two sampled beams, namely, two scanning points; we assume one scanning point equates to one measurement in Stage 2. Thus, when the S-curve interpolation process repeat L times, the number of total measurements of the DS-BA method is

$$M_{total} = M^2_{scan} + 2 \times 4L. \tag{28}$$

2) Total Complexity: The computational complexity shows how many flops are needed to complete the alignment [18], [19]. In Stage 1, the complexity of implementing $N_{active} \times N_{active}$ phase-shifting matrix at both Tx and Rx, for Stage y, where $y \in [1, 2]$, is given by [18], [19]

$$C^{\text{y}}_{p-af} = 10N^2_{active} \times M_{Tx} + 10N^2_{active} \times M_{Rx}. \tag{29}$$

Considering the element pattern for pattern multiplication, the calculation of element pattern increases the complexity as [18]

$$C^{\text{y}}_{\text{ep}} = \frac{5}{2} M_{Tx} \log_2(M_{Tx}) + \frac{5}{2} M_{Rx} \log_2(M_{Rx}). \tag{30}$$

Subsequently, we come to calculate radiation intensities, and then antenna gains. The complexity of this process turns to

$$C^{\text{y}}_{\text{ap}} = 8(M_{Tx} + M_{Rx}). \tag{31}$$

After obtaining antenna gains for all scanning points, the generation of table matrices will introduce extra complexity

$$C^{\text{y}}_{\text{table}} = 3M_{tot}. \tag{32}$$

Here, $M_{Tx} = M_{Rx} = M_{scan}$ with $M_{tot} = M^2_{scan}$ in Stage 1 for both methods and $M_{tot} = M_{Tx} M_{Rx}$ in Stage 2 for the DD-BA method. Thus, total complexity of the DD-BA method is

$$C_{\text{total}} = \sum\nolimits_{y=1,2} (C^{\text{y}}_{p-af} + C^{\text{y}}_{\text{ep}} + C^{\text{y}}_{\text{ap}} + C^{\text{y}}_{\text{table}}). \tag{33}$$

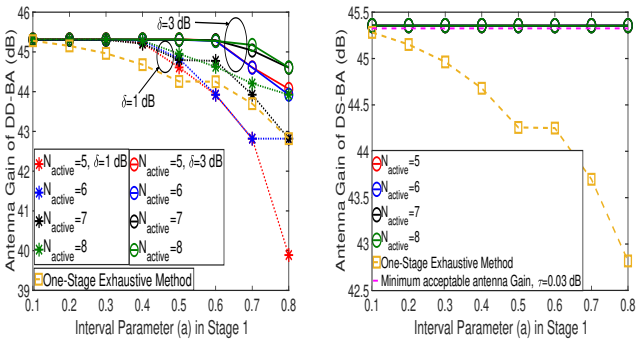

Fig. 5: Antenna Gain $G_{max}\ (dB)$ vs. Interval parameter a in Stage 1. $\tau = 0.03\ dB$ in the DS-BA method.

The DS-BA method operates (29)-(31) with $M = 2$ and $N_{active} = N$ in Stage 2. The linear interpolation requires four flops [20]. If the S-curve interpolation repeat L times, the total complexity is given by

$$C_{\text{total}} = C^1_{p-af} + C^1_{\text{ep}} + C^1_{\text{ap}} + C^1_{\text{table}} + 4L(20N^2 + 25). \tag{34}$$

V. Numerical Results

Our setup involves an 8×8-element antenna array. For deactivating approach, $N^2_{active}/N^2 \geq 1/3$ is required to obtain a satisfactory performance [17]. The values of AoD and AoA are randomly selected from $[-5, 5]$ (deg) to evaluate the average performance by Monte-Carlo simulation. The sample interval is $\Delta = 5$ (deg) and all initial scan ranges are $[-15, 15]$ (deg). The interval parameter in Stage 2 is $b = 0.05$. The parameters of the experimental communication link are given in Table I.

Fig. 5 shows the achievable antenna gain vs. the interval parameter a in Stage 1, in which both DD-BA and DS-BA methods can outperform the conventional one-stage exhaustive method. In Fig. 5 (a), the DD-BA method can obtain the achievable antenna gain matching the maximum value, in the region of $a \leq 0.3$. Nevertheless, the achievable antenna gain drops rapidly when $a > 0.3$ with $\delta = 1(dB)$ and $a > 0.6$ with $\delta = 3(dB)$. Moreover, the DS-BA method shown in Fig. 5 (b), can always meet the antenna gain requirement. This is because Step 5 in Stage 2 guarantees that the required gain loss $\tau = 0.03\ (dB)$ will be satisfied. According to these results, the DS-BA method could be considered as a close-to-optimal beam alignment method to certainly achieve the antenna gain requirement by exploiting the theoretical beam pattern.

TABLE I: Parameters of Experimental Communication Link

Parameters	
Inter-antenna Distance D	3.15 mm
mmWave frequency f	47.619 GHz
Normalised inter-antenna distance d	0.5
Tx power	18.0 dBm
Tx-Rx Distance	500 m
Path loss	-123.6 dB
$G_{opt} = G^{TX}_{ANT} + G^{RX}_{ANT}$	45.3213 dB
Minimum Rx Power	-80 dBm
Acceptable Gain loss	$\tau \leq 19.7213$ dB

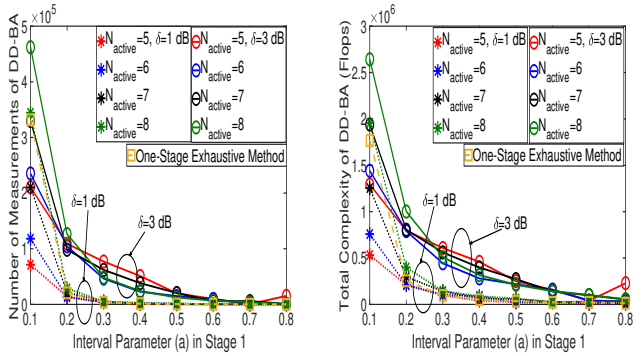

Fig. 6: a) Number of Measurements and b) Total complexity vs. Interval parameter a in Stage 1 of the DD-BA method

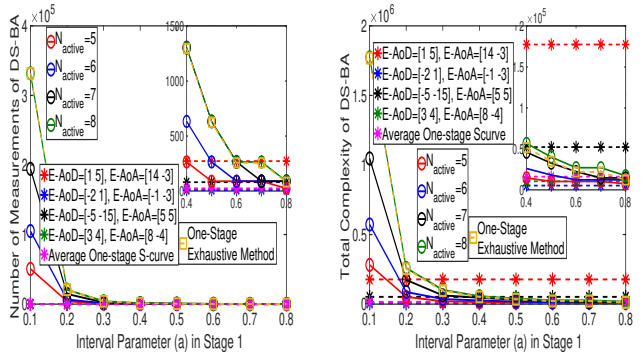

Fig. 7: a) Number of Measurements and b) Total complexity vs. Interval parameter a in Stage 1 of the DS-BA method, $\tau = 0.03$ dB, AoD=[0 2] and AoA=[-4 1] for One-stage S-curve method.

The number of measurements and total complexity of DD-BA and DS-BA methods are shown in Fig. 6 and Fig. 7. Both DD-BA and DS-BA methods can outperform the conventional one-stage exhaustive method. Fig. 6 shows that in the DD-BA method, a smaller δ (dB) benefits the measurement and complexity reductions because it leads to a narrower scan range for Stage 2. Thus, by tuning a and δ (dB) properly, the DD-BA method can offer measurement/complexity reduction while satisfying the required antenna gain. From Fig. 7, we can observe that DS-BA offers reduced measurements and complexity compared to DD-BA. Moreover, "E-" in the legends indicates the randomly estimated directions. The results of the one-stage S-curve method (i.e. applying the S-curve approach without a preceding coarse beam scanning) with AoD=[0 2] and AoA=[-4 1] indicate that the linear interpolation to S-curve helps to closely match the optimal AoD and AoA. However, the S-curve interpolation might repeat $L > 1$ times if smaller $\tau(dB)$ is required, or the estimated directions are outside the main lobe range. Thus, the randomness of the estimated directions affects the number of measurements and complexity. It shows the DS-BA method outperforms the one-stage S-curve method, especially when N_{active} and a are small because the deactivating approach can guarantee the estimated directions are in the main lobe range and leads to $L = 1$ so that Stage 2 will be processed only once. Therefore, $N_{active} = 5$ and $a = 0.8$ can be selected for DS-BA to attain the required antenna gain with the minimum measurements and complexity.

VI. Conclusion

This paper has studied the design of low-complexity two-stage beam alignment methods in LOS mm-wave systems. The DD-BA method achieves coarse steering in Stage 1 by deactivating antennas and relatively fine steering in Stage 2. The DS-BA method obtains the estimated directions in Stage 1 by deactivating antennas and utilizes them to complete the beam-pattern assisted S-curve interpolation. Our numerical results have demonstrated that the proposed methods could attain the target of antenna gain satisfaction and avail measurement/complexity reductions with properly selected parameters.

References

[1] S. Haghighatshoar and G. Caire, "The beam alignment problem in mmwave wireless networks," in *Proc. 50th ACSSC*, 2016, pp. 741–745.

[2] M. Hussain and N. Michelusi, "Energy-efficient interactive beam alignment for millimeter-wave networks," *IEEE Trans. Wireless Commun.*, vol. 18, no. 2, pp. 838–851, 2019.

[3] R. W. Heath *et al.*, "An overview of signal processing techniques for millimeter wave MIMO systems," *IEEE J. Sel. Topics Signal Process.*, vol. 10, no. 3, pp. 436–453, 2016.

[4] J. Song *et al.*, "Adaptive millimeter wave beam alignment for dual-polarized mimo systems," *IEEE Trans. Wireless Commun.*, vol. 14, no. 11, pp. 6283–6296, 2015.

[5] S. Hur *et al.*, "Millimeter wave beamforming for wireless backhaul and access in small cell networks," *IEEE Trans. Commun.*, vol. 61, no. 10, pp. 4391–4403, 2013.

[6] Z. Xiao *et al.*, "Hierarchical codebook design for beamforming training in millimeter-wave communication," *IEEE Trans. Wireless Commun.*, vol. 15, no. 5, pp. 3380–3392, 2016.

[7] J. Wang *et al.*, "Beam codebook based beamforming protocol for multi-gbps millimeter-wave wpan systems," *IEEE J. Sel. Areas Commun.*, vol. 27, no. 8, pp. 1390–1399, 2009.

[8] D. Zhang *et al.*, "Exploring AoA/AoD dynamics in beam alignment of mobile millimeter wave MIMO systems," *IEEE Trans. Veh. Technol*, vol. 68, no. 6, pp. 6172–6176, 2019.

[9] A. Alkhateeb *et al.*, "Channel estimation and hybrid precoding for millimeter wave cellular systems," *IEEE J. Sel. Topics Signal Process.*, vol. 8, no. 5, pp. 831–846, 2014.

[10] C. Liu *et al.*, "Millimeter wave beam alignment: Large deviations analysis and design insights," *IEEE J. Sel. Areas Commun.*, vol. 35, no. 7, pp. 1619–1631, 2017.

[11] G. A. T. Warren L. Stutzman, *Antenna Theory and Design*. John Wiley & Sons, Inc., Hoboken, New Jersey., 2012.

[12] S. V. Hum, "Radio and Microwave Wireless Systems," *University of Toronto.*, 2007.

[13] H. Friis, "A note on a simple transmission formula," *Proceedings of the IRE*, vol. 34, no. 5, pp. 254–256, 1946.

[14] C. A. Balanis, "Antenna theory: Analysis and design," *John Wiley & Sons, Inc., Hoboken, New Jersey.*, 2005.

[15] J. Carl B. Dietrich, *Adaptive Arrays and Diversity Antenna Configurations for Handheld Wireless Communication Terminals*. Academic Press, 2000.

[16] R. A. Monzingo and T. W. Miller, *Introduction to Adaptive Arrays*. New York, NY:John Wiley & Sons Inc.,, 1980.

[17] A. Garcia-Rodriguez and C. Masouros, "Exploiting the increasing correlation of space constrained massive MIMO for CSI relaxation," *IEEE Trans. Commun.*, vol. 64, no. 4, pp. 1572–1587, 2016.

[18] M. Arakawa, "Computational workloads for commonly used signal processing kernels," *DTIC Document, Project Rep. SPR-9, Mass. Inst. Technol., Cambridge, MA, USA,*, 2006.

[19] H. Yang and T. L. Marzetta, "Performance of conjugate and zero-forcing beamforming in large-scale antenna systems," *IEEE J. Sel. Areas Commun.*, vol. 31, no. 2, pp. 172–179, 2013.

[20] O. Guven *et al.*, "Computationally efficient real-time interpolation algorithm for non-uniform sampled biosignals," *Healthcare Technology Letters*, vol. 3, pp. 105 – 110, 2016.